Resonant states in $GaAs/Ga_{1-X}Al_XAs$ Multi-Quantum-Wells

M. Hammouchi , A. Bousfia, E.H. El Boudouti and A. Nougaoui
Laboratoire de Dynamique et d'Optique des Matériaux, Département de Physique, Faculté des Sciences, Université Mohamed Premier, Oujda, Morocco

B. Djafari-Rouhani, M.L.H. Lahlaouti, A. Akjouj, and L. Dobrzynski
Laboratoire de Dynamique et Structure des Matériaux Moléculaires, U.R.A. CNRS 801, UFR de Physique, Université de Lille 1, 59 655 Villeneuve d'Ascq, France.

The effect of buffer layers on resonant states in a Multi-Quantum-Well (MQW) sandwiched between two substrates, is investigated here theoretically. These resonances appear as well-defined peaks in the density of states (DOS). The local and total density of states are obtained from an analytical determination of the Green functions. Due to the substrate/buffer layer/ MQW /substrate interaction, different kinds of resonant states are found and their properties are investigated. We show in particular that an incident electron in the left-hand side substrate is transmitted in the right hand side substrate of the structure with large time delays in the phase time. The peaks in the phase time associated with the transmission coefficient are found to be similar to those corresponding to the DOS. The intensity of these peaks associated with extended states in MQW's and Tamm like states lying at the MQW/buffer layer interface, strongly depends on the width of the buffer layer.

The electronic structure of a Multi-Quantum-Well (MQW) with n-wells consists of the formation of n-level energy[1-3] because of the coupling between adjacent wells. Furthermore, with periodic potential of very large n eventually approachs the band model. For an infinite periodic potential in Kronig-Penny model[4], there is formation of energy minibands separated each other by minigaps[3] whose widths and positions are characteristic of the layer sequence. If the periodic structure is interrupted by having a buffer potential barrier higher or lower than that in the bulk superlattice (SL)[5-8], or by having the last well wider or narrower than the rest[9-12], localised states occur in the forbidden bands. These states are called surface states or Tamm states[13]. Because of the presence of the substrate barrier at the outermost of a quantum structure, this surface state presents a bound character. The resonance behaviour of the tunnelling exists when the substrate barrier, which serves as a support for the devices, is lower than barriers in the rest of the quantum structure (MQW). The resonant-tunnelling is studied in earlier works, first the resonant-tunnelling diode[3,14] in double barriers structure, the resonant-tunnelling bipolar transistor[15], triple-barrier structure[16-22], quadriple-structures[23] and multibarrier tunnelling[24,25]. However in all these studies, the surface states have not been dealt in resonant-tunnelling structure.

In a previous work, we have dealt with resonant states in a single quantum-well structure[26]. The aim of this work was to investigate the effect of the size and the nature of the mediums surrounding the quantum well. In this communication, we are dealing with a more complicated structure which consists on a MQW sandwiched between two substrates with an embedded buffer layer (Fig.1). The latter structure is different from the former one and presents new

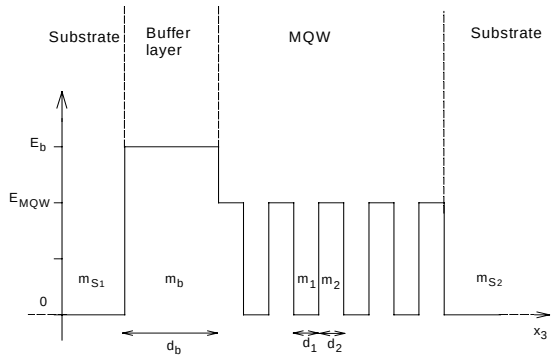

Fig.1 : Potential profile representation of a MQW (with 4 wells and 5 barriers) sandwiched between two substrates with an embedded buffer layer. d_1, d_2, and d_b are, respectively, the thickness of the well, the barrier and the buffer layers. E_b and E_{MQW} are, respectively, the barrier heights of the buffer layer and the MQW. m_1, m_2, m_b, m_{S1}, and m_{S2} are, respectively, the effective-mass of the well, the barrier, the buffer and the two substrates S_1 and S_2.

features because of the existence of minibands separated by minigaps. Different kinds of resonant states induced by the MQW/buffer layer in the continuum of the substrate bulk bands are investigated. In particular, resonant states localised at the interface between the MQW and the buffer layer (called Tamm states) are found.

The Green's function is calculated by using the interface response theory[27] in composite materials in which the solution is first searched in the restricted space of the interfaces before being extended to the whole material. As a consequence, our system becomes equivalent to a simple linear chain with a pseudoatom located at each interface of the MQW. The Green's function approach enables us to calculate the local and total density of states (DOS), and allows us also to determine the transmission and reflection rates as well as the phase times. The phase time is considered[28] to be relevant physical time to describe the motion of wave packets narrow in wave-number space. There are several other times[29-31], however the only well-defined and well-established one[30] is the 'dwell time' which is the average time spent in a given region by all incoming particles. We show that the positions of the resonances obtained from DOS coincide with those given by phase time and transmission rate. The half widths of the peaks in the DOS and phase time are related to the lifetime of the resonant states. We avoid the detail of the analysis which is similar to that of Ref. [32] and only report the expressions of the total DOS and the transmission rate as well as the phase time in the appendix.

In the following we give a few illustrations related to a MQW deposited on a buffer layer of different material than those in the MQW, and the whole system is bounded by two substrates. The MQW is modelled by a finite bilayer superlattice (SL) with the surrounding layers being of barrier type (see Figure 1). The thicknesses d_1 and d_2 of the layers in the MQW are assumed to be equal.

For numerical calculations, the $Al_xGa_{1-x}As$-based system has been chosen, as it exhibits excellent growth characteristics and enables one to realise and to manipulate a wide range of potential profiles. In such a structure, the potential barrier height and the effective-masse value for a given region are determined by the Al mole fraction x_i in the corresponding $Al_{xi}Ga_{1-xi}As$ semiconductor (i=1,2 for the MQW layers, i = b for the buffer layer and i = S_1 and i = S_2 for the two substrates). These quantities are given by[5]: $E_i(x_i) = 944x_i$ meV and $m_i(x_i) = (0.067 + 0.083\ x_i)\ m_{el}$, respectively, m_{el} being the free-electron mass (after Ref. 5).

Figure 2 gives the variation of the electronic energy levels versus the buffer layer thickness of the system depicted in Figure 1. To this purpose, all the other structure parameters are fixed, in particular, the number of layers composing the MQW (4 wells and 5 barriers) and the Al concentrations: x_1=0 (in the layer 1 made of the GaAs well) and x_2 = 0.4 (in the layer 2 made of the $Al_{0.4}Ga_{0.6}As$ barrier). This results in the effective masses and potential barriers: $m_1=0.067m_{el}$, $m_2= 0.1002m_{el}$,V_1=0 and V_2= 377.6meV. The thicknesses of the layers are taken to be equal to 40Å. The MQW with the buffer barrier is sandwiched between two GaAs substrates (see Fig.1). The potential barrier height of the buffer layer is chosen to be higher than the MQW potential barriers, namely, x_b=0.6 (buffer layer made of $Al_{0.6}Ga_{0.4}As$ barrier) with $m_b= 0.1168m_{el}$ and V_b= 566.4meV. The potential profile is sketched in figure 1.

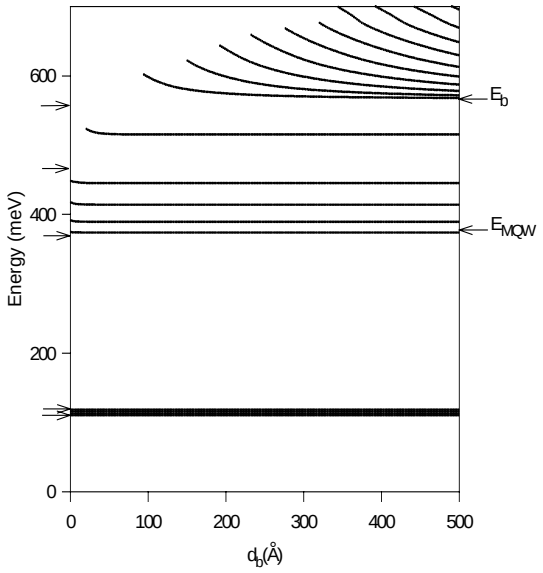

Fig. 2: Variation of the energy levels of resonant states as a function of the thickness of the buffer layer barrier. The arrows in the left axis give the SL minibands edges and the arrows in the right axis indicate the heights barriers E_{MQW} and E_b of the MQW and the buffer layer respectively.

All the branches in figure 2 represent resonant states induced by the buffer/MQW system in the continuum of the bulk bands of the GaAs substrates. These resonant states are obtained from the maxima of the DOS, shown in figure 3 for a few values of the thickness d_b. The arrows in the left axis of Fig.2 give the limits of the infinite superlattice (SL) minibands and the arrows in the right axis indicate the potential barrier heights of the MQW (E_{MQW}) and of the buffer layer (E_b) respectively. All the curves situated below E_b represent resonant states of the MQW, and appear as well defined peaks in the DOS of figure 3 even

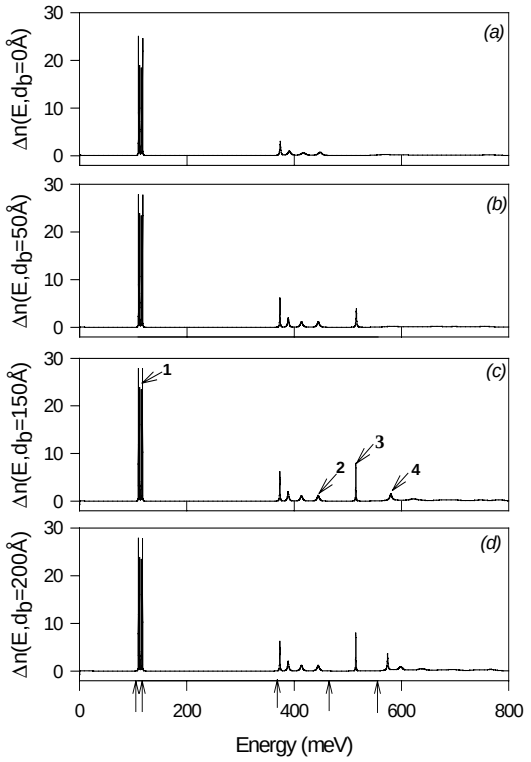

Fig. 3: Variation of the DOS versus the energy for d_b=0 (a), d_b=50Å (b), d_b=150Å (c) and d_b=200Å (d). The vertical arrows at the bottom axis energy correspond to the limits of the bulk bands.

though they are in resonance with the bulk states of the surrounding substrates. The corresponding energies of these resonances present a small variation with d_b (see figure 2), and the number of states inside each miniband reflects the number of wells constituting the MQW (in this example, we have 4 wells). However, the states lying in the first bulk band are very sharp and belongs to the quantum wells (see Fig. 4(a)) as their energies lie below the MQW barrier, while the states lying in the second bulk band are broadened and belongs to the whole MQW (see Fig. 4(b)) as their energies lie above the MQW barrier. It is well known that in such heterostructure, due to the coupling between adjacent GaAs wells, there is formation of discrete energies whose width and position are characteristic of the layer sequence, and for large number of wells, the discrete levels form a quasi-continuous miniband[3,24]. The alone state lying in the forbidden band above the second miniband (see figure 2) represents the internal surface state induced by the presence of the buffer layer potential barrier as it is illustrated in figure 4(c). This internal surface state is a resonant state and appears as well defined peak in the DOS of figure 3 for $d_b \neq 0$ (see the mode labelled 3 in Fig.3(c)). Moreover, the intensity of this internal surface state increases with the thickness d_b of the $Ga_{0.4}Al_{0.6}As$ buffer layer and for large values of d_b, the intensity of the internal surface state remains constant. On the other hand, the energy level of the internal surface state is considerably affected by the buffer layer barrier height (not given here) namely, either the level and the intensity of this state decrease when the buffer layer barrier height decreases. Concerning the curves lying above E_b in figure 2, they present a noticeable variation when d_b increases and tend asymptotically to the limit of E_b when $d_b \rightarrow \infty$. These resonances correspond to waves with predominant amplitude in the buffer barrier (see below), even though they are propagating in the whole system.

An analysis of the local DOS as function of the space position x_3 (figure 4) clearly shows the localisation properties of the differente kind of states belonging to different energy range. The local DOS reflects the spatial behaviour of the square modulus of the wave function (i.e., the charge distribution). Figures 4(a) and (b) correspond to the states respectively labelled 1 and 2 in figure 3(c), showing that these resonances are confined in the MQW. Figure 4(c) correspond to the resonant state labelled 3 in figure 3(c), showing that this state is confined at the MQW/buffer layer interface and decays on both sides of this interface as its energy

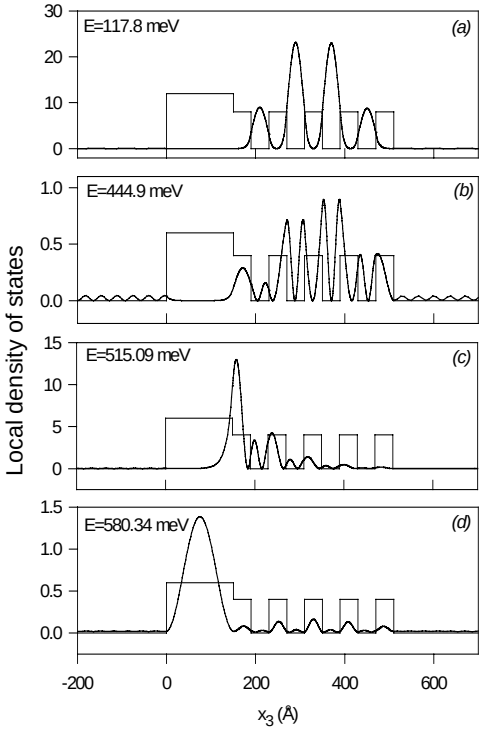

Fig. 4: Spatial representation of the local DOS for E=117.8meV (a), E=444.9meV (b), E=515.09meV (c) and E=580.34meV, for a given buffer layer thickness (d_b=150Å).

lies in the minigap region. Vertical and horizontal lines represent the potential profile. The existence of such a state is induced by the broken symmetry of the MQW equal barrier sequence; furthermore, the wave function will be partially reflected by the $Ga_{0.4}Al_{0.6}As/Ga_{0.6}Al_{0.4}As$ interface. This is quit similar to the case of a thin transparent slab with one side coated with semi-reflection mirror material, where the incident light will form some quasistationary wave at some special wavelengths. Figure 4(d) corresponds to the state labelled 4 in figure (3c), showing that this resonance rather belongs to the buffer layer barrier. In the continuum of the whole system, the electron confinement is almost predominant in the barriers. A similar behaviour was found for electrons in a single quantum well[26], a quantum step[33], MQW[34], excitons[35], optical waves[36], where above barrier states are localised in the barrier rather than in the well regions. In figure 5, we illustrate the transmission rate versus the energy for some few values of the buffer layer thickness d_b. For d_b=0, if the energy of an incident electron coincides with a resonant state, the electron is completely transmitted. Figure 5 shows clearly that the transmission rate decreases with d_b (figures 5(b) and 5(c)) and for large value of d_b (figure 5(d)), only the continuum states of the whole system (above E_b) are transmitted. Thus, by increasing d_b, the buffer layer barrier prevents more and more the tunnelling of electron waves through the MQW leading to the lake of informations in the transmission rate about resonant states below E_b. In this case, only the phase time gives us informations on the interaction of an incident electron with the resonant states confined in the MQW below E_b. Indeed, for a better characterisation of these resonant states, we give in figure 6 a comparison of all the quantities cited above (DOS and phase time) for two values of the buffer layer thickness: d_b =0 (figures 6(a) and 6(b)) and d_b =150Å (figures 6(c) and 6(d)).

In figure 6, the DOS and the phase time give both the same behaviour. Indeed, the full width at half maximum of the peaks in these two latter quantities is related to the finite lifetime of the resonant states in relation with the uncertainty principle. Meanwhile, the intensity of the peaks in the DOS gives the weight of the resonances, while the intensity of the peaks in the phase time describes the time needed for electron to complete the transmission process. The transmission phase time is interpreted as the delay motion of the electron to appear in the substrate lying on the right-hand side of the buffer layer/MQW device.

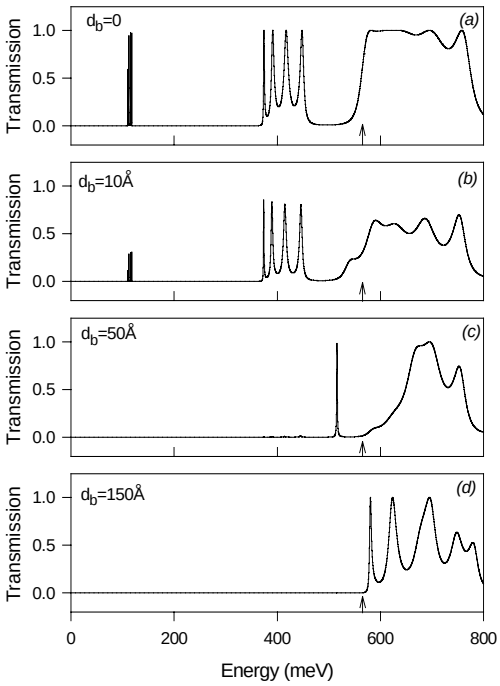

Fig. 5: The transmission rate versus the energy for d_b=0 (a), d_b=10Å (b), d_b=50Å (c) and d_b=150Å (d). The arrows indicate the potential barrier height E_b of the buffer layer.

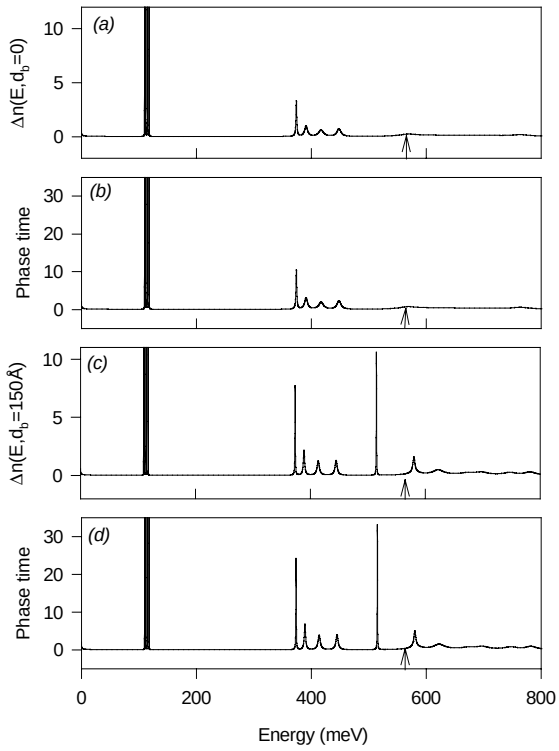

Fig. 6: Energy dependence of the DOS (a) and (c), and the transmitted phase time (b) and (d) for d_b=0 ((a) and (b)), and d_b=150 ((c) and (d)).The arrows indicate the potential barrier height E_b of the buffer layer.

In conclusion, a complete and closed-form expressions for the local and total DOS were obtained (see the appendix). These expressions enable us to derive the dispersion of resonant states for electronic energy levels in the substrate/buffer layer/MQW/substrate system taking into account in this structure, the effect of the size and the height of the buffer layer barrier separating the MQW and the substrate as well as the effect of this latter material which serves as a support for the device. We have also calculated the transmission rate and the transmitted phase time expressions. The transmitted phase time present similar behaviour as the DOS versus the energy and both quantities are better characterising the resonances than the transmission rate. The transmission rate quantity show that the buffer layer barrier may prevents some electron waves from tunnelling through the MQW when its thickness becomes large. This result show that the buffer layer barrier is of considerable interest of optimising the energy window for resonant tunnelling and control surface-related phenomena in mesoscopic systems. The observation of the resonant tunneling states through such MQW's studied here may be possible via the measurement of a current and a conductance versus an applied voltage[38,39].

As a final remark, let us mention that the different results presented in this work will not be probably affected by taking into account the non-parabolicity effect. Indeed, it has been shown[40] that the effect of the non-parabolicity on the electronic structure of GaAs-GaAlAs MQW's is negligible and so can be the transmission rate and the DOS.

ACKNOWLEDGMENT

The work of M. H, A.B., E. E. and A. N. has been supported by the Program-in-Aid for Scientific Research (PARS).

APPENDIX

Each material i (i=1,2) in the SL is characterised by its effective-masse m_i, the potential barrier height E_i and thickness d_i. Similarly the buffer layer and the two substrates involve, respectively, the parameters (m_b,, d_b , E_b) and (m_{Si} , E_{Si} *(i=1,2)).*

Let us first define the following parameters in each material ***i = 1, 2, b, S_1, S_2***

$$C_i = ch\alpha_i d_i \quad , \quad S_i = sh\alpha_i d_i \quad ,$$

$$F_i = \frac{2}{2m_i}\alpha_i$$

$$\alpha_i^2 = -\frac{2m_i}{2}(E - E_i) \qquad \text{with} \quad i = 1, 2, b, S_1, S_2$$

$$R = \frac{1 + \dfrac{F_b S_b}{F_{S1} C_b}}{1 + \dfrac{F_{S1} S_b}{F_b C_b}} \quad ,$$

and

$$t = exp(ik_3 D)$$

In particular, the bulk dispersion relation in the infinite MQW [37] is

$$cos(k_3 D) = C_1 C_2 + \frac{1}{2}\left(\frac{F_1}{F_2} + \frac{F_2}{F_1}\right) S_1 S_2 \ .$$

Then we introduce four specific quantities, namely, Y_1^S and Y_2^S corresponding to the MQW/Substrate interface on one side, and Y_1^b and Y_1^b associated with the embedded buffer layer on the other side:

$$Y_1^S = C_1 C_2 + \frac{F_1}{F_2} S_1 S_2 - t - F_{S_2}\left(C_1 \frac{S_2}{F_2} + C_2 \frac{S_1}{F_1}\right) ,$$

$$Y_2^S = C_1 - C_2 t - F_{S_2}\left(\frac{S_1}{F_1} + \frac{S_2}{F_2} t\right) \ ,$$

$$Y_1^b = C_1 C_2 + \frac{F_1}{F_2} S_1 S_2 - t - RF_{S_1}\left(C_1 \frac{S_2}{F_2} + C_2 \frac{S_1}{F_1}\right) ,$$

$$Y_2^b = C_1 - C_2 t - RF_{S_1}\left(\frac{S_1}{F_1} + \frac{S_2}{F_2} t\right) \ .$$

The expression of the total density of states can be written as the sum of five contributions

$$n(E) = n_1(E) + n_2(E) + n_b(E) + n_{S1}(E) + n_{S2}(E)$$

where $n_1(E)$ and $n_2(E)$ are the contributions of layers 1 and 2 of the SL, respectively, and $n_b(E)$, $n_{S1}(E)$ and $n_{S2}(E)$ come, respectively, from the buffer layer and the two substrates. Actually, in the two latter terms, we subtract the contribution of the bulk of the two substrates, which are an infinite quantities and write $n_{Si}(E) = n_B(E) + \Delta n_{Si}(E)$ *(i=1,2).*

$$n_1(E)=$$

$$-\frac{1}{\pi}Im\frac{t}{t^2-1}\left\{\frac{t(1-t^{2N})}{(t^2-1)}\frac{Y}{\Delta^-}\left[\frac{d_1S_2}{2F_2}\left(1-\frac{F_2^2}{F_1^2}\right)+\frac{S_1}{\alpha_1F_1}\left(C_2S_1+\frac{1}{2}C_1S_2\left(\frac{F_2}{F_1}+\frac{F_1}{F_2}\right)\right)\right]\right. \tag{A1}$$

$$\left.+\frac{N\Delta^+}{\Delta^-}\left[\frac{S_1S_2}{2\alpha_1F_2}\left(1-\frac{F_2^2}{F_1^2}\right)+\frac{d_1}{F_1}\left(C_2S_1+\frac{1}{2}C_1S_2\left(\frac{F_2}{F_1}+\frac{F_1}{F_2}\right)\right)\right]\right\}\quad,$$

$$n_2(E)=$$

$$-\frac{1}{\pi}Im\frac{t}{t^2-1}\left\{\frac{(1-t^{2N+2})}{(t^2-1)}\frac{Y}{\Delta^-}\left[\frac{d_2S_1}{2F_1}\left(1-\frac{F_1^2}{F_2^2}\right)+\frac{S_2}{\alpha_2F_2}\left(C_1S_2+\frac{1}{2}C_2S_1\left(\frac{F_2}{F_1}+\frac{F_1}{F_2}\right)\right)\right]\right. \tag{A2}$$

$$\left.+\frac{(N+1)\Delta^+}{\Delta^-}\left[\frac{S_1S_2}{2\alpha_2F_1}\left(1-\frac{F_1^2}{F_2^2}\right)+\frac{d_2}{F_2}\left(C_1S_2+\frac{1}{2}C_2S_1\left(\frac{F_2}{F_1}+\frac{F_1}{F_2}\right)\right)\right]\right\}\quad,$$

$$n_b(E)=$$

$$-\frac{1}{2\pi}Im\frac{1}{\Delta^-}\frac{1}{\left(1+\frac{F_{S_1}S_b}{F_bC_b}\right)}\left\{\left(\frac{t^2-1}{t}+Y_1^S\right)\left\{\frac{S_b}{\alpha_bC_b}\left[\left(\frac{C_1S_2}{F_2}+\frac{C_2S_1}{F_1}\right)+\frac{F_{S_1}}{F_b^2}\left(\frac{t^2-1}{t}+Y_1^s\right)\right]\right.\right.$$

$$+d_b\left[\left(\frac{C_1S_2}{F_2}+\frac{C_2S_1}{F_1}\right)-\frac{S_b}{F_bC_b}\left(\frac{t^2-1}{t}+Y_1^s\right)+\frac{F_{S_1}}{F_b^2}\left[\frac{F_bS_b}{C_b}\left(\frac{C_1S_2}{F_2}+\frac{C_2S_1}{F_1}\right)\right.\right. \tag{A3}$$

$$\left.\left.\left.-\left(\frac{t^2-1}{t}+Y_1^S\right)\right]\right]\right\}-t^{2N}Y_2^S\left\{\frac{S_b}{\alpha_bC_b}\left[\frac{S_1}{F_1}+\frac{S_2}{F_2}t+\frac{F_{S_1}}{F_b^2}(C_1+C_2t)\right]+d_b\left[\frac{S_1}{F_1}+\frac{S_2}{F_2}t-\right.\right.$$

$$\left.\left.\left.\frac{S_b}{F_bC_b}(C_1+C_2t)+\frac{F_{S_1}}{F_b^2}\left[\frac{F_bS_b}{C_b}\left(\frac{S_1}{F_1}+\frac{S_2}{F_2}t\right)-(C_1+C_2t)\right]\right]\right\}\right\}$$

and

$$\Delta n_{S_1}(E)=-\frac{1}{\pi}Im\frac{1}{2\alpha_{S_1}}\left[\frac{1}{2F_{S_1}}+\frac{1}{\Delta^-}\frac{1}{\left(1+\frac{F_{S_1}S_b}{F_bC_b}\right)}\left\{\left(\frac{t^2-1}{t}+Y_1^S\right)\left[\left(\frac{C_2S_1}{F_1}+\frac{C_1S_2}{F_2}\right)\right.\right.\right.$$

$$\left.\left.\left.-\frac{S_b}{F_bC_b}\left(\frac{t^2-1}{t}+Y_1^S\right)\right]-t^{2N}Y_2^S\left[\frac{S_1}{F_1}+\frac{S_2}{F_2}t-\frac{S_b}{F_bC_b}(C_1+C_2t)\right]\right\}\right]\quad, \tag{A4}$$

$$\Delta n_{S_2}(E)=-\frac{1}{\pi}Im\frac{1}{2\alpha_{S_2}}\left[\frac{1}{2F_{S_2}}+\frac{1}{\Delta^-}\left\{\left(\frac{t^2-1}{t}+Y_1^b\right)\left(\frac{C_2S_1}{F_1}+\frac{C_1S_2}{F_2}\right)\right.\right.$$

$$\left.\left.-t^{2N}Y_2^b\left(\frac{S_1}{F_1}+\frac{S_2}{F_2}t\right)\right\}\right]\quad, \tag{A5}$$

where

$$Y = \left(\frac{t^2 - 1}{t} + Y_1^S \right) Y_2^b + \left(\frac{t^2 - 1}{t} + Y_1^b \right) Y_2^S$$

and

$$\Delta^{\pm} = \left(\frac{t^2 - 1}{t} + Y_1^S \right) \left(\frac{t^2 - 1}{t} + Y_1^b \right) \pm t^{2N} Y_2^S Y_2^b .$$

The poles of the Green's function give the localised waves, namely,

$$\Delta^{-} = 0 \quad .$$

Consider a wave function of incident electrons in the substrate S_1 (see figure 1) represented by the plane wave $e^{-\alpha_S x_3}$ of unit amplitude. The incident electrons are scattered from the interfaces between dissimilar layers constituting the system. The amplitude of transmitted electrons $C_T(E)$ in the substrate S_2 is expressed as

$$C_T(E) = -2F_{S_1} \frac{t^N}{\Delta^{-}} \frac{t^2 - 1}{t} \frac{\frac{S_1}{F_1} + \frac{S_2}{F_2} t}{C_b \left(1 + \frac{F_{S_1} S_b}{F_b C_b} \right)},$$

The transmission rate T is written as

$$T = \left| \frac{F_{S_2}}{F_{S_1}} \right| |C_T(E)|^2 \qquad \text{(A6)}$$

The phase time, i.e. the time that it takes the peak of an electron packet to appear in the right-hand-side substrate medium is given, in the stationary phase approximation, by

$$\tau_T = \frac{d\theta_T}{dE}, \qquad \text{(A7)}$$

where $h = 2\pi$ is the Plank's constant and θ_T is the phase of the transmitted amplitude of electrons in the right-hand-side substrate (Fig.1).

---

[1]L. Esaki and R. Tsu, IBM Res. Devlop. **14**, 61 (1970)

[2]L. L. Chang, L. Esaki, W. E. Howard, and R. Ludeke, J. Vac, Sci. Technol. **10**, 11 (1973)

[3]R. Tsu and L. Esaki, Appl. Phys. Lett. **22**, 562 (1973).

[4]R. de. L. Kronig and W. G. Penny, Proc. R. Soc. London A **130**, 499 (1930)

[5]H. Ohno, E. E. Mendez, J. A. Brum, J. M. Hong, F. Agullo-Rueda, L. L. Chang, and L. Esaki Phys. Rev. Lett, **64**, 2555 (1990) ; H. Ohno, E. E.Mendez, A. Alexandrou, J. M. Hong, Surf. Sci. **267**, 161 (1992)

[6]F.Y. Huang, App. Phys. Lett. **57**, 1669 (1990)

[7]W. Blosss, Phys. Rev. B **44**, 8035 (1991)

[8]S. Fafard Phys. Rev. B **50,** 1991 (1994)

[9]L. Pavesi, E. Tuncel, B. Zimmerman, and F. K. Reinhart, Phys. Rev. B **39** 7788 (1989)

[10]F. Agullo-Rueda, E. E.Mendez, H. Ohno, and J. M. Hong, Phys. Rev. B **42**, 1470 (1990)

[11]R. Kucharczyk and M. Steslicka Solid State commun., **81**, 557 (1992)

[12]H. K. Sy and T. C. Chua, Phys. Rev. B **48,** 7930 (1993)

[13]I. Tamm, Phys. Z. Sov. **1**, 733 (1932)

[14]L. L. Chang, L. Esaki, and R. Tsu, Appl. Phys. Lett. **24,** 593 (1974)

[15]F. Capasso and R. A. Kiel, J. Appl. Phys. **58**, 1366 (1985)

[16]M. C. Payne, J. Phys. C **18**, L879 (1985)

[17]T. Nakagawa *et al*, Appl. Phys. Lett., **49**, 73 (1986)

[18]K. Araki, J. Appl. Phys. **62**, 1059 (1987)

[19]H. Yamamato, and Y. Kanie, Phys. Status Solidi B **160**, K97 (1990)

[20]H. Yamamato, Y. Kanie, and K. Taniguchi, Phys. Status Solidi B **167**, 597 (1991)

[21]D. X. Xu *et al.* , J. Appl. Phys. **71**, 3859 (1992)

[22]D. Bertram, H. T. Grahm, C. Van Hoof, J. Genoe, G. Borghs, W. W. Rühle, and K. Von Klitzing, Phys. Rev. B **50**, 17 309 (1994)

[23]H. Yamamato, Y. Kanie, and K. Taniguchi, Phys. Status Solidi B **162**, K25 (1990)

[24]X. W. Liu and A. P. Stamp, Phys. Rev. B **47**, 16 605 (1993), **50**, 1588 (1994)

[25]A. J. Shields, C. Tralleo-Giner, M. Cardona, H. T. Grahn. K. Ploog, V. A. Haisler, D. A. Tenne, N. T. Moshegov, and A. I. Toropov, Phys. Rev. B **46**, 6990 (1992)

26M. Hammouchi, E.H. El Boudouti, A. Nougaoui, and B. Djafari-Rouhani, J. Phys.: Condens. Matter, **10**, 2039 (1998)

[27]L. Dobrzynski, Surf. Sci. Rep. **11**, 139 (1990) ; J. Mendialdua, T. Szwacka, A. Rodriguez and L. Dobrzynski, Phys. Rev. B **39**, 10 674 (1989) ; **37**, 8027 (1988)

[28]E. H. Hauge, J. P. Falck, T. A. Fjeldly, Phys. Rev B **36,** 4203 (1987)

[29]E. H. Hauge and J. A. Stõveng, Rev. Mod. Phys. **61,** 917 (1989)

[30]G. Iannaccone and B. Pellegrini, Phys. Rev B **49,** 16 548 (1994) and references therein

[31]R. Landauer and Th. Martin Rev. Mod. Phys. **66**, 217 (1994)
[32]M. Hammouchi, E. H. El Boudouti, A. Nougaoui, B. Djafari-Rouhani, M. L. H. Lahlaouti, A. Akjouj, and L. Dobrzynski, Phys. Rev. B **59**, 1999 (1999) ; M. L. H. Lahlaouti, A. Akjouj, B. Djafari-Rouhani, L. Dobrzynski, M. Hammouchi, E. H. El Boudouti, and A. Nougaoui, J. Opt. Soc. Am. A, 16, (1999)
[33]See, for example : W. Lu, Y. M. Mu, X. Q. Liu, X. S. Chen, M. F. Wan, G. L. Shi, Y. M. Qiao, S. C. Shen, Y. Fu, and M. Willander Phys. Rev. B **57**, 9787 (1998)
[34]See, for example: T. Worren, K. B. Ozanyan, O. Hunderi, and F. Martelli, Phys. Rev. B **58**, 3977 (1998); M. Jaros and K.B. Wong J. Phys. C: Solid State Phys. **17**, L765 (1984); M. Babiker and B.K. Ridley Superlatt. Microstruct. **2**, 287 (1986)
[35]See, for example: F. C. Zhang, H. Dai, N. Luo, N. Samarth, M. Dobrowolska, J. K. Furdyna, and L. R. Ram-Mohan Phys. Rev. Lett. **68,** 3 220 (1992)
[36]See, for example: M. L. Bah, A. Akjouj, E. H. El Boudouti, B. Djafari-Rouhani and L. Dobrzynski, J. Phys. : Condens. Matter **8,** 417 (1996)
[37]R. E. Camley, B. Djafari-Rouhani L. Dobrzynski, and A. A. Maradudin, Phys. Rev. B **27**, 7318 (1983)
[38]L. L. Chang, L. Esaki, and R. Tsu, Appl. Phys. Lett. **24**, 593 (1974)
[39]L. Esaki and L. L. Chang, Phys. Rev. Lett. **33,** 495 (1974)
[40]D. Ait el Habti, Morr. J.: Condens. Matter **1**, 1, 103 (1998) and references therein